NASA/CR—2002-211866

APEX 3D Propeller Test Preliminary Design

Anthony J. Colozza
Analex Corporation, Brook Park, Ohio

September 2002

The NASA STI Program Office . . . in Profile

Since its founding, NASA has been dedicated to the advancement of aeronautics and space science. The NASA Scientific and Technical Information (STI) Program Office plays a key part in helping NASA maintain this important role.

The NASA STI Program Office is operated by Langley Research Center, the Lead Center for NASA's scientific and technical information. The NASA STI Program Office provides access to the NASA STI Database, the largest collection of aeronautical and space science STI in the world. The Program Office is also NASA's institutional mechanism for disseminating the results of its research and development activities. These results are published by NASA in the NASA STI Report Series, which includes the following report types:

- TECHNICAL PUBLICATION. Reports of completed research or a major significant phase of research that present the results of NASA programs and include extensive data or theoretical analysis. Includes compilations of significant scientific and technical data and information deemed to be of continuing reference value. NASA's counterpart of peer-reviewed formal professional papers but has less stringent limitations on manuscript length and extent of graphic presentations.

- TECHNICAL MEMORANDUM. Scientific and technical findings that are preliminary or of specialized interest, e.g., quick release reports, working papers, and bibliographies that contain minimal annotation. Does not contain extensive analysis.

- CONTRACTOR REPORT. Scientific and technical findings by NASA-sponsored contractors and grantees.

- CONFERENCE PUBLICATION. Collected papers from scientific and technical conferences, symposia, seminars, or other meetings sponsored or cosponsored by NASA.

- SPECIAL PUBLICATION. Scientific, technical, or historical information from NASA programs, projects, and missions, often concerned with subjects having substantial public interest.

- TECHNICAL TRANSLATION. English-language translations of foreign scientific and technical material pertinent to NASA's mission.

Specialized services that complement the STI Program Office's diverse offerings include creating custom thesauri, building customized databases, organizing and publishing research results . . . even providing videos.

For more information about the NASA STI Program Office, see the following:

- Access the NASA STI Program Home Page at *http://www.sti.nasa.gov*

- E-mail your question via the Internet to help@sti.nasa.gov

- Fax your question to the NASA Access Help Desk at 301–621–0134

- Telephone the NASA Access Help Desk at 301–621–0390

- Write to:
  NASA Access Help Desk
  NASA Center for AeroSpace Information
  7121 Standard Drive
  Hanover, MD 21076

NASA/CR—2002-211866

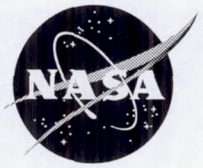

APEX 3D Propeller Test Preliminary Design

Anthony J. Colozza
Analex Corporation, Brook Park, Ohio

Prepared under Contract NAS3–00145

National Aeronautics and
Space Administration

Glenn Research Center

September 2002

Trade names or manufacturers' names are used in this report for identification only. This usage does not constitute an official endorsement, either expressed or implied, by the National Aeronautics and Space Administration.

The Aerospace Propulsion and Power Program at NASA Glenn Research Center sponsored this work.

Available from

NASA Center for Aerospace Information
7121 Standard Drive
Hanover, MD 21076

National Technical Information Service
5285 Port Royal Road
Springfield, VA 22100

Available electronically at http://gltrs.grc.nasa.gov

Table of Contents

System

There have been a number of recently proposed scientific missions that require subsonic aircraft to fly within a very low Reynolds number flight regime. These air vehicles include both Earth-based high altitude atmospheric research vehicles as well as aircraft to fly within the atmospheres of other planets such as Mars. One of the most efficient ways to generate thrust for a low speed aircraft is through a propeller. However the generation of appreciable thrust from a propeller under such very low atmospheric densities conditions, requires the propeller to operate at high RPM levels where an appreciable portion of the blade tip sees transonic flow. There is little aerodynamic data for the operation of airfoils within the low Reynolds number, high Mach number flight environment, which will be encountered by the propeller.

The 3D-propeller experiment will investigate the operation of a propeller under such low Reynolds number, high Mach number flight conditions. The propeller will be instrumented to determine performance under these flight conditions. A block diagram of the main components of the proposed propeller experiment is shown in Figure 1.

The experiment would be carried upon the APEX vehicle as a piggyback experiment. A nacelle will be installed on a faring above the fuselage canopy. The proposed orientation of the experiment is shown in Figure 2. The experiment will operate in the following manner (listed in Table 1) throughout the launch and flight of the APEX vehicle.

TABLE 1.—PROPELLER EXPERIMENT OPERATION OVERVIEW

Flight Phase [1]	APEX Vehicle [1]	Propeller Experiment
Ascent	Balloon Launch and Ascent to 33 km (108 kft) approximately 2 hours duration	Propeller is locked during ascent using a mechanical breaking system.
Launch	Release from the balloon	The breaking system is released allowing the propeller to begin to spin up to speed. Data acquisition system is turned on and control data begins to be collected.
Transition to Flight	Leveling Rocket Fires Vehicle sees Highest G Loading	The RPM is monitored and breaking is applied as needed to maintain RPM below the critical limit for the propeller.
Test Maneuvers	Flight Maneuvers are Performed, Vehicle Descends from 31 km (102 kft) to 21 km (70 kft) altitude	Electric motor is engaged and the propeller spins up to desired RPM. Testing is performed over a range of RPM's as the vehicle descends through the test altitude range. Approximately 20 minutes of test time is performed.
Descent / Landing	Vehicle glides from the end of the test altitude to landing	The propeller windmills for the decent. Breaking is used if necessary to maintain propeller RPM below critical levels.

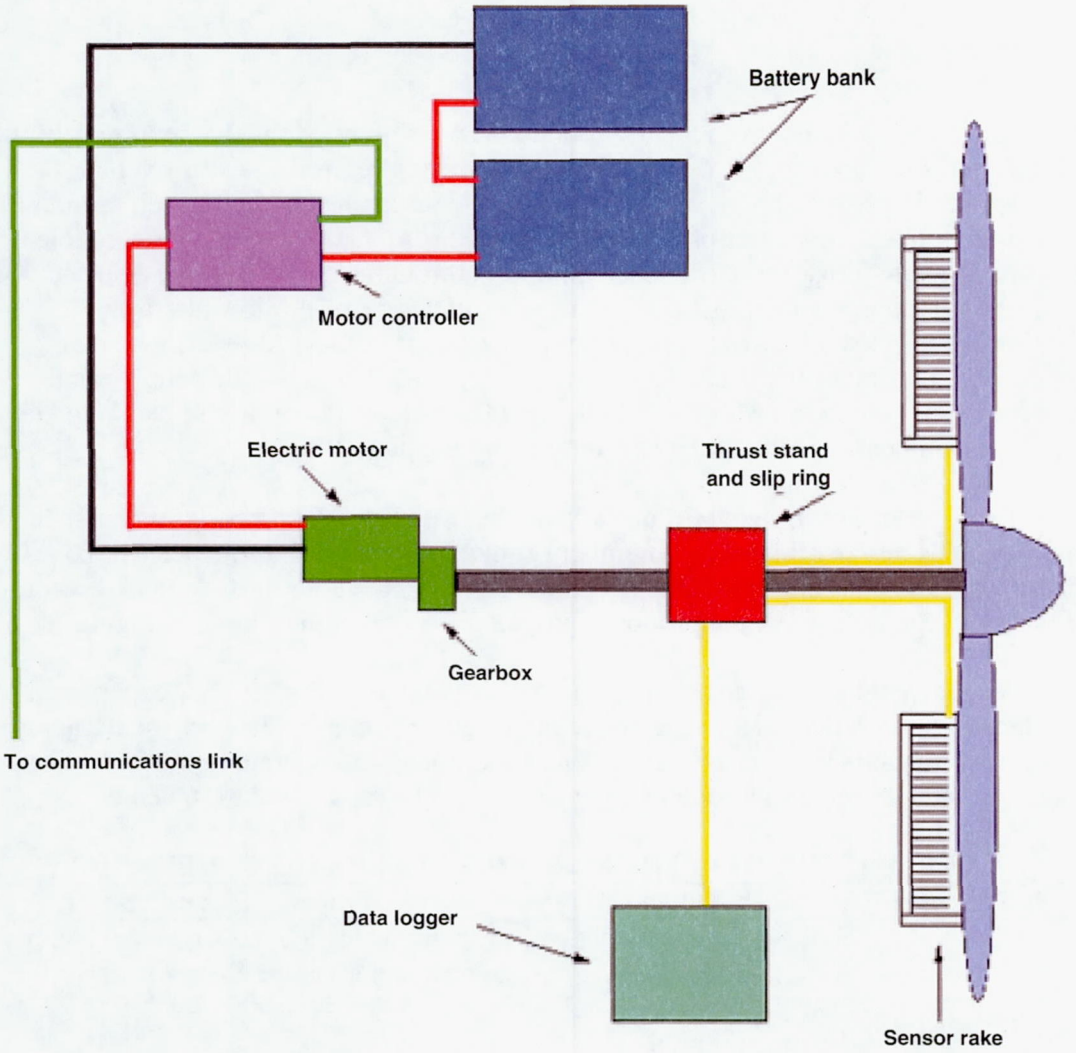

Figure 1 Propeller System Test Layout

The preliminary design for the 3D propeller experiment is an iterative process between the various components necessary in the system. Component selection not only establishes the particular capabilities of a given component but effects the required performance of the other components in the system. For example, the capabilities of the electric motor that was chosen will effect the maximum RPM and torque available. Also, the battery capability will determine power available and test duration. For the preliminary design an initial pass was made evaluating each component and determining its performance, capabilities and requirements. The propeller design point and system components were selected because they should be capable of operating together and achieving the test requirement goals. In order to produce an operational system, compromises on the performance of individual components had to be made. A further refinement of this design through the iteration process will be performed in the Phase II

portion of the project. The Phase II portion of the project will also include a detailed design and construction of the system described in this Phase I report.

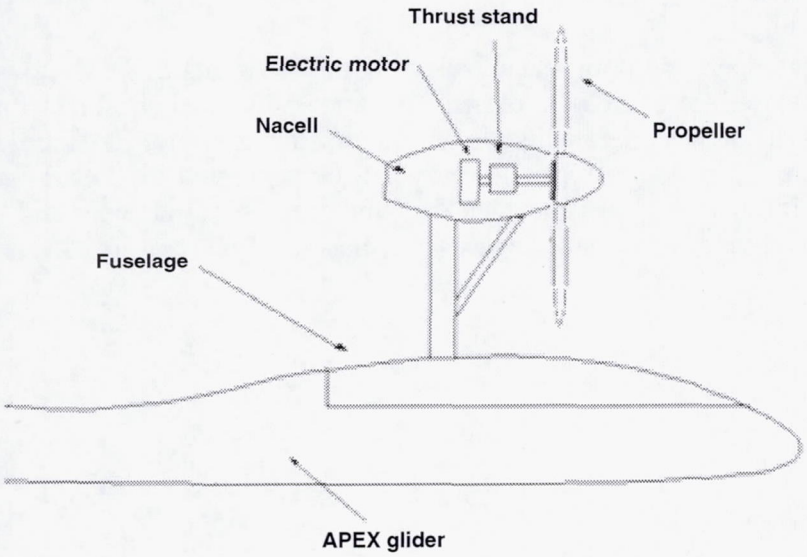

Figure 2 Orientation of Propeller Experiment on APEX Vehicle

Propeller

The propeller design has to meet the requirements of operating under the required flight conditions as well as conforming to any physical and safety constraints imposed by the APEX vehicle itself.

For this preliminary design, a vortex theory code with low Reynolds number corrections was used to generate the estimated performance. The airfoil selected for the propeller was the SD8000-PT low Reynolds number airfoil [2]. This airfoil was chosen because of its very good lift-to-drag characteristics at low Reynolds numbers as well as its post stall lift generation capability. A curve of lift coefficient (C_l) vs drag coefficient (C_d) and C_l versus angle of attack (α), at a Reynolds number of 60,000 are shown in Figures 3 and 4. The geometry of the airfoil is shown in Figure 5 and its coordinate points are given in Appendix A.

The propeller was assumed to be a fixed pitch propeller. This was done to reduce the complexity of the system. However, with a fixed pitch propeller, some capability and performance had to be sacrificed. It had to be determined what the best operating blade

angle was for the propeller. The blade angle is akin to various gearing ratios in a car. The higher the blade angle (or gear) the lower the operational RPM (for a given thrust) but the greater the torque required. The geometry of the propeller, which includes the twist and the variation of chord with radius, is shown in Figure 6. The pitch angle specified for the blade represents the angle the blade is at the 3/4 radius point. The diameter of the propeller was chosen to be 1.5 m. This was the largest diameter that could be reasonably placed on the APEX vehicle.

Determining the operating point meant selecting the blade angle, RPM, power required and thrust generated. The selection of these parameters was also influenced by the capabilities of the other components of the system, such as motor RPM and battery power available. Propeller performance curves were generated for both 2 and 4 bladed propellers at altitudes of 31 km and 21.5 km which represent the upper and lower test altitude ranges. These performance curves are shown in Figures 7 to 10.

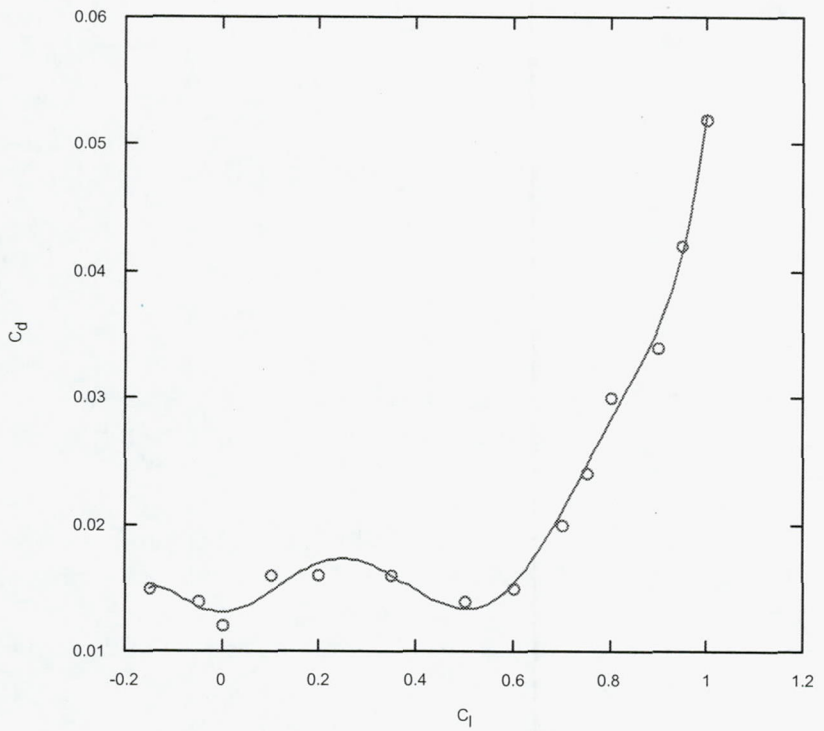

Figure 3 C_l versus C_d for SD8000-PT airfoil at 60,000 Re, M < 0.1[2]

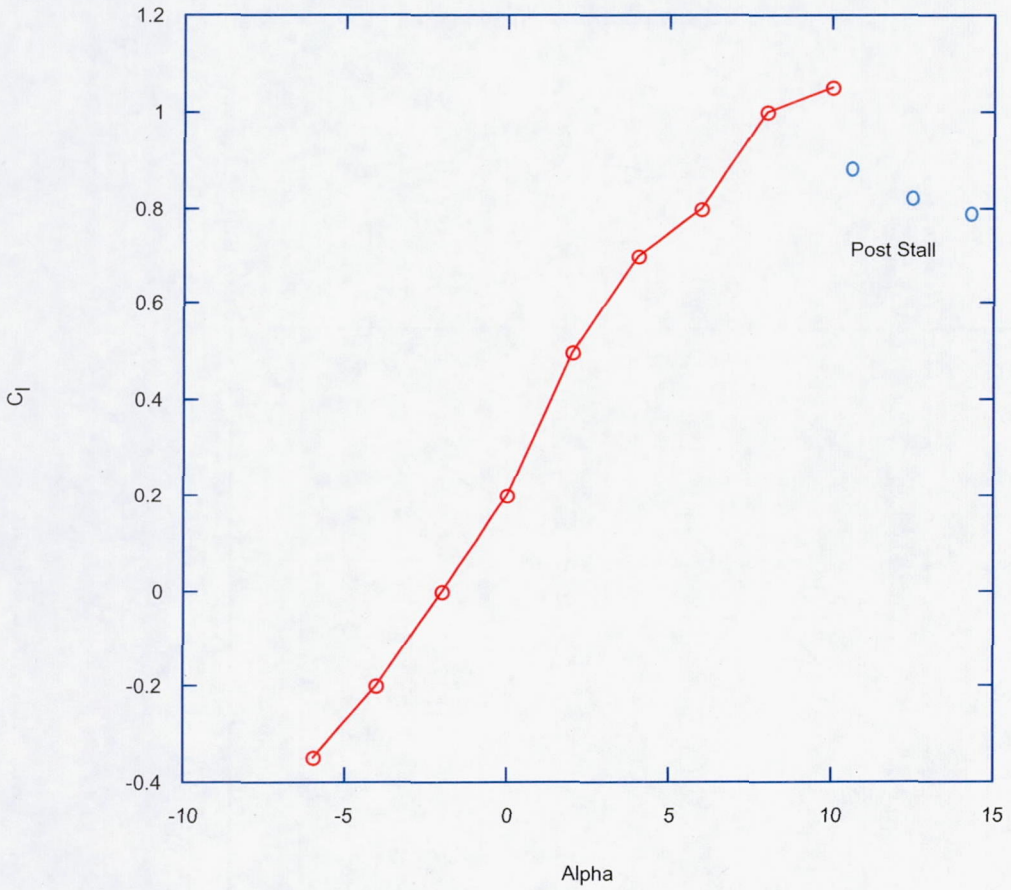

Figure 4 C_l versus Alpha for SD8000-PT airfoil at 60,000 Re [2]

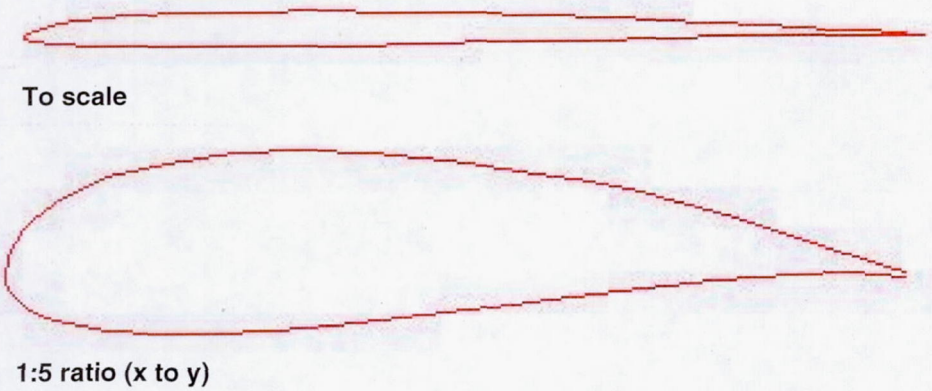

Figure 5 SD8000-PT Airfoil Cross Section

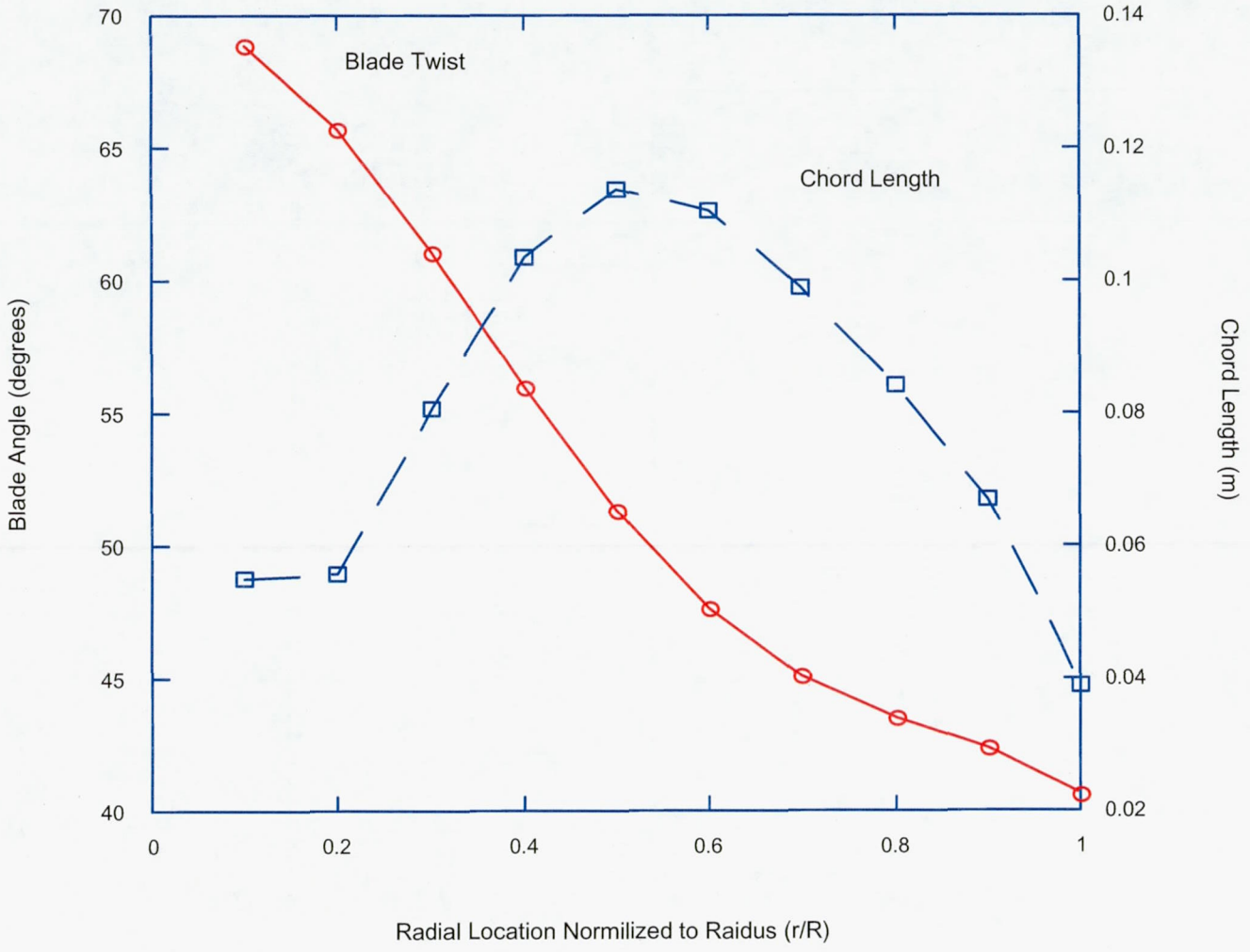

Figure 6 Propeller Blade Twist and Chord Length

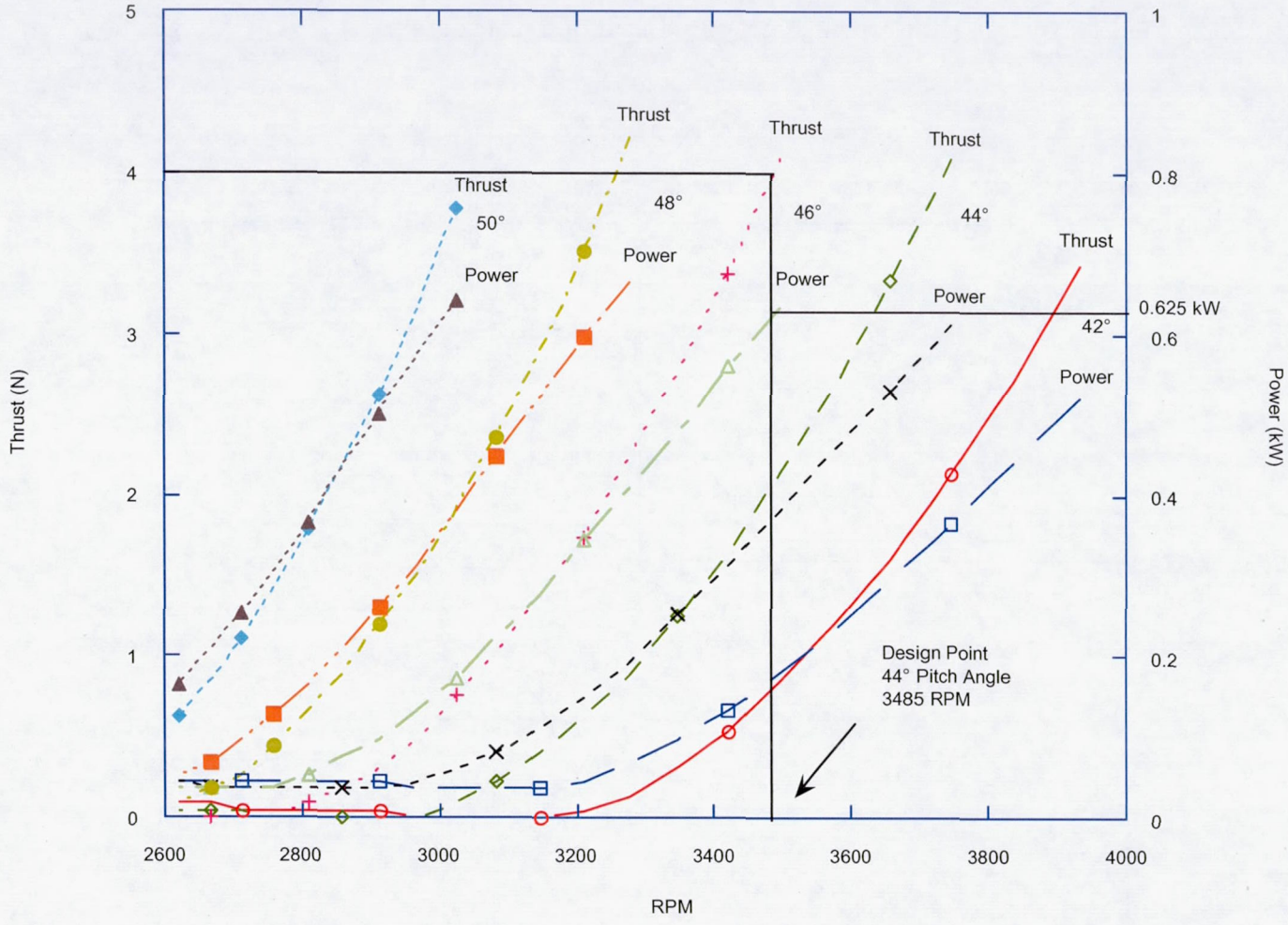

Figure 7 Two Bladed Propeller Performance 31 km Altitude, flight Mach Number of 0.5

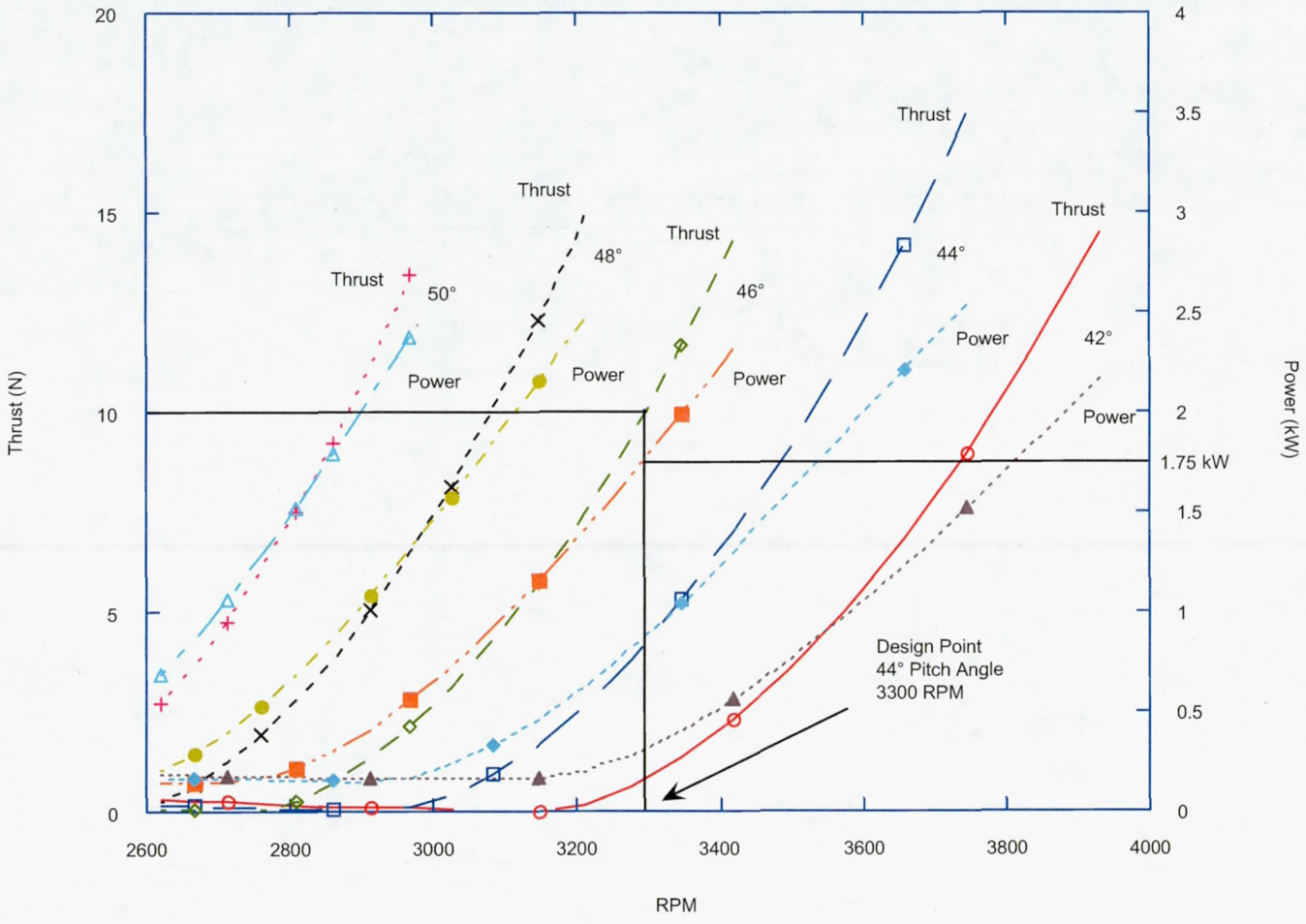

Figure 8 Two Bladed Propeller Performance 21.5 km Altitude, flight Mach Number of 0.5

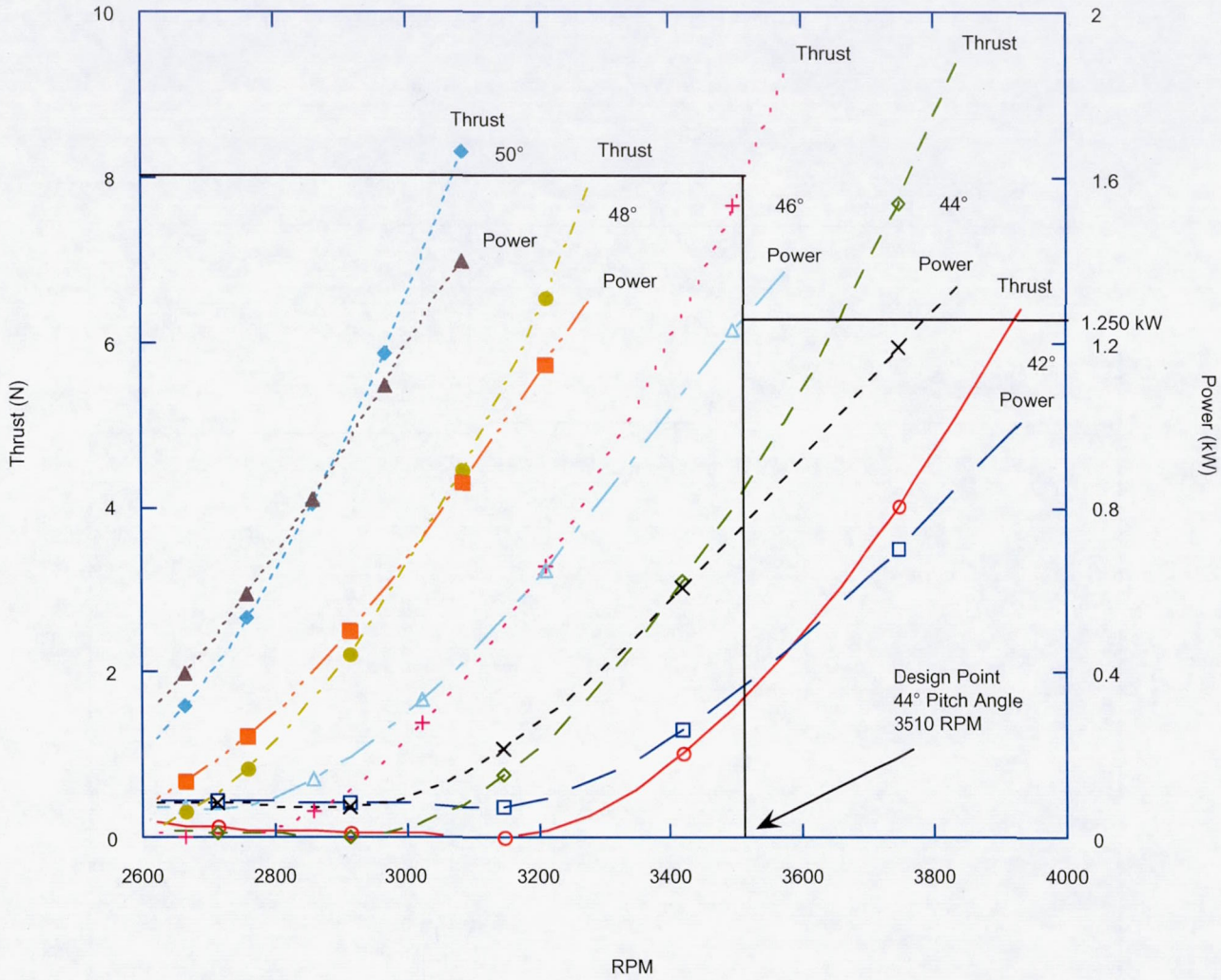

Figure 9 Four Bladed Propeller Performance 31 km Altitude, flight Mach Number of 0.5

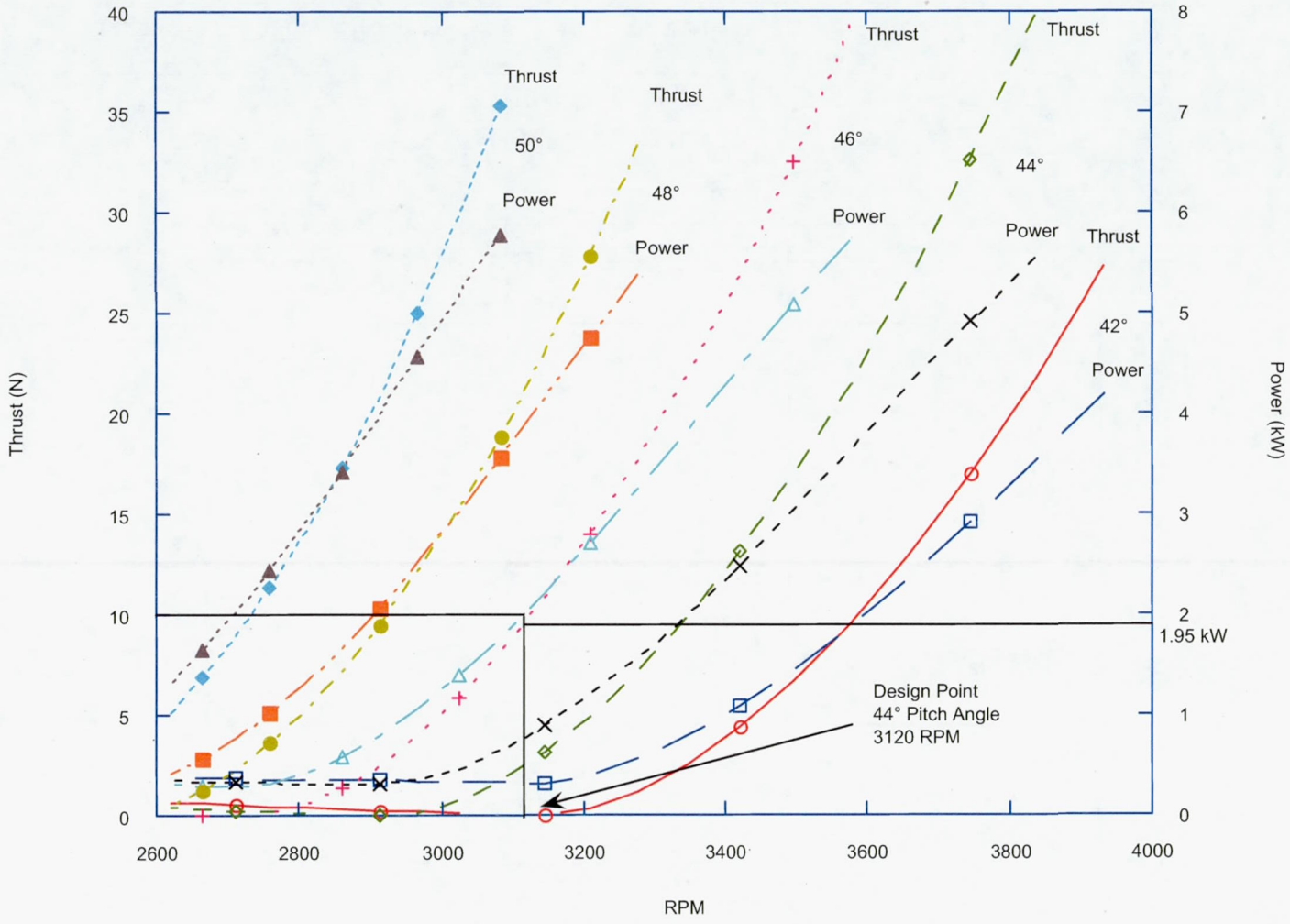

Figure 10 Four Bladed Propeller Performance 21.5 km Altitude, flight Mach Number of 0.5

The operational conditions for both the 2 and 4 bladed propellers is given in Table 2. Based on this information in combination with the battery and electric motor selections, it was determined that the 2 bladed propeller design would be more appropriate for this experiment. Although the thrust level is lower at the starting altitude, the reduced power consumption as well as the lower required motor torque enable a much lighter system. Also the propeller weight is reduced by the elimination of two of the propeller blades.

TABLE 2.—PROPELLER PERFORMANCE CHARACTERISTICS AT THE DESIGN POINT

# Blades	Altitude (km)	RPM	Efficiency	Torque (N-m)	Thrust (N)	Shaft Power (kW)
2	31.0	3485	93%	1.900	4	0.625
2	21.5	3300	81%	5.616	10	1.750
4	31.0	3510	93%	3.771	8	1.250
4	21.5	3120	72%	6.619	10	1.950

A detailed design and performance map will be produced for the propeller within the Phase II portion of the program. It is planned to make the propeller as stiff and structurally strong as possible. Although this doesn't represent how an actual lightweight high altitude propeller would be constructed, it does present a number of advantages for this type of experiment. Mainly, it dramatically reduces the design cost and effort by eliminating the need for a detailed structural model of the propeller. By making the propeller stiff there is no change in its shape when under loading. Therefore this increases the accuracy of comparing the predicted performance to the actual performance since the blade shape is no longer a variable during operation. Also it reduces the risk of the experiment by utilizing a structurally rigid propeller that is much less likely to fail during operation. The only drawback to this approach is the addition of weight due to the rigid propeller blades. However, this is minimal due to the thinness of the blades and therefore should not have a significant effect on the total system weight.

The propeller will operate at various RPM values throughout the flight. As the density and RPM change, the operational Reynolds number will also change. Figure 11 shows how the Reynolds number will change during the flight. The Reynolds number range predicted at the 3/4 station along the blade is 31,700 to 147,000.

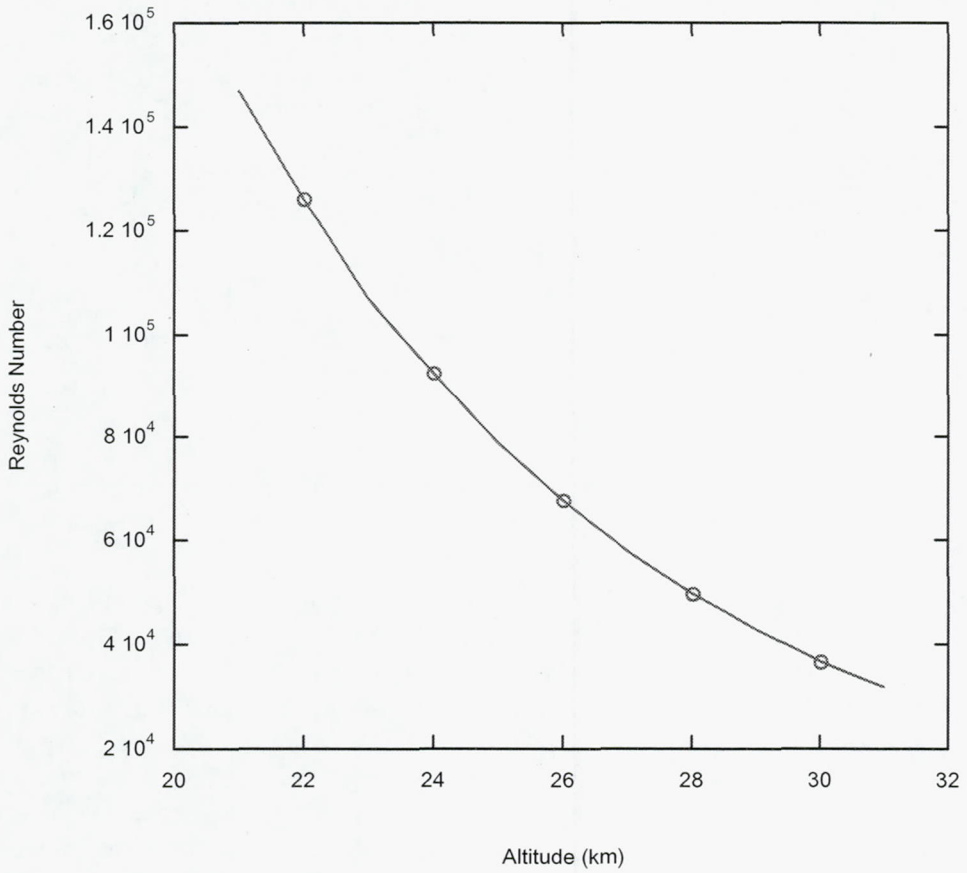

Figure 11 Propeller Operational Reynolds Number at 3/4 Blade Station

Structurally, the propeller is a cantilevered beam fixed at the hub with a distributed load over its surface. To keep it as light as possible a carbon composite will be used. This material also provides tremendous structural strength. An approximate blade loading profile is shown in Figure 12. Because the aerodynamic loading is fairly small (a maximum of 10 N under power at altitude) the largest force on the propeller will be due to the centrifugal loading applied due to rotation. The overall loading of the blade in the plane of rotation can be somewhat controlled by utilizing this centrifugal loading. Any deflection in the blade due to thrust will cause the blade to bend slightly out of the plane of rotation. This provides a moment arm for the centrifugal force normal to the plane of rotation to pull the blade back toward the plane of rotation. This interaction of the centrifugal force should be sufficient, under the loading conditions expected, to sustain the blade within the plane of rotation.

If desired, the blade could also be designed to compensate for any determined bending moment due to loading. This is done by slightly tilting the blade out of the plane of rotation, thereby providing a component of the centrifugal force normal to the plane of rotation. If the expected bending moment is known, the tilt given to the blade and corresponding force generated could offset the thrust bending moment and significantly reduce the net moment felt by the blade.

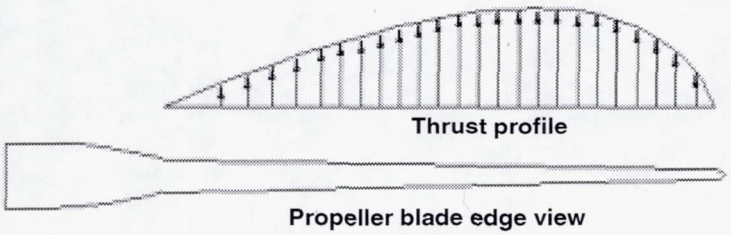

Figure 12 Typical Thrust Profile Over the Length of the Propeller Blade

Based on the airfoil shape and the chord distribution, shown in Figures 5 and 6, the total volume of each blade was calculated to be 421 cm^3. Based on this volume, the estimated blade mass is 0.58 kg per blade (1.16 kg for both blades) if constructed with carbon fiber (density of 1350 kg /m^3) and 1.18 kg per blade (2.36 kg for both blades) if constructed with a high strength aluminum alloy (2014-T6, 4.4% Cu, density of 2800 kg/m^3). For these mass estimates the tangential loading on the blade will be on the order of 26 MPa for the carbon blade and 53 MPa for the titanium blade. This is well below the yield points of 3500 MPa and 825 MPa respectively for each material.

Battery

A battery is the source of power for the propeller during the experiment. The battery must be capable of providing the amount of power needed to meet the thrust and torque requirements of the propeller. Because of the relatively short duration of the testing and the fairly large amount of power required the battery must be capable of discharging at a high rate, approximately 3C. (A 1C discharge rate means that the battery will fully discharge in 1 hour, 3C is one third of an hour).

To allow for repeated test runs and reduce cost, only rechargeable or secondary batteries were considered for use. The total number of runs will depend on the number of propeller

blade geometries to be tested as well as the number of desired blade angles for each. The two candidate batteries selected for this application are a conventional Nickel Cadmium (NiCd) battery and a more current Lithium Ion (Li-Ion) battery. These battery packs are shown in Figure 13.

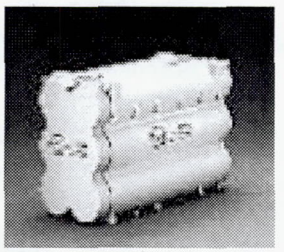

Figure 13 Saft NiCd Battery Pack [3] Saft Li-Ion Battery Back [3]

The NiCd batteries are off-the-shelf with an established history and readily available whereas the Li-Ion batteries are a newer technology and custom made. The Li-Ion batteries cost about two to three times as much as the NiCd batteries. However, their main advantage is that they weigh about 1/2 as much as the NiCd battery and take up less volume (as shown below). Both batteries will be sized for this application since the tradeoff between cost, weight, volume and acceptable risk will be addressed under the Phase II portion of the program. Since both types of batteries are sealed and do not require air for their operation, the low air pressure environment will not effect their performance.

The total watt-hours that the battery must supply is approximately 383 W-hrs. This is shown as the area under the curve in Figure 14. For analysis purposes, this value assumes a linear increase in power from the 600 watts needed at 31km to the 1700 watts needed at 21.5 km. It also assumes that the propeller will be running for 20 minutes over this altitude range. These assumptions are on the conservative side and therefore allow some margin to be built into the battery sizing.

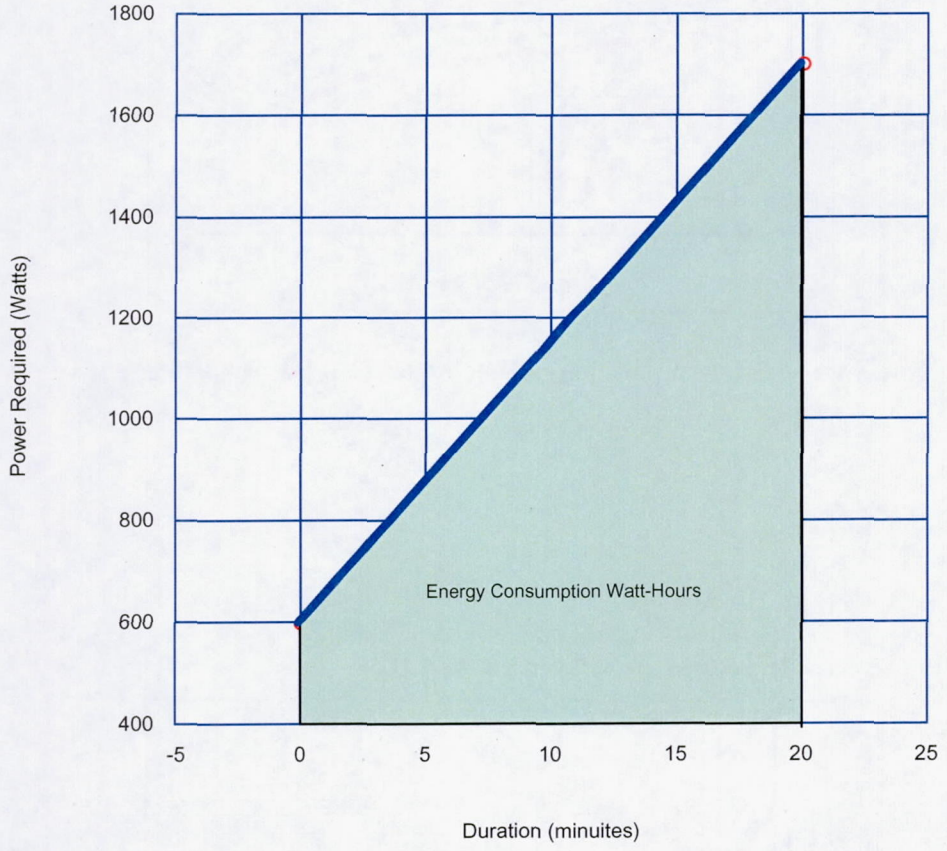

Figure 14 Power Required During Experiment

The two main factors that effect the ability of the batteries to provide this energy level are depth of discharge (how much of the total energy stored in the battery is discharged) and the discharge or C-rate. The effect of these factors on the batteries performance are shown in Figures 15 and 16 for a Saft, Inc. STM Ni-Cad battery and Figures 17 and 18 for a Saft, Inc. Li-Ion battery. [3]

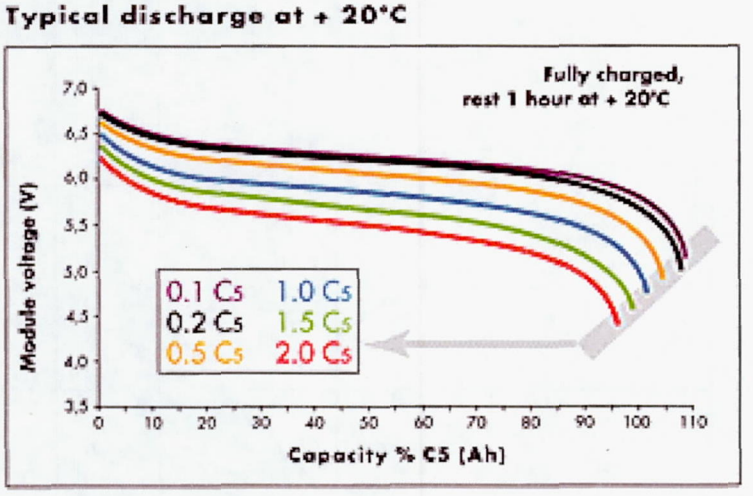

Figure 15 Effect of Discharge Rate on Ni-Cad Battery Voltage [3]

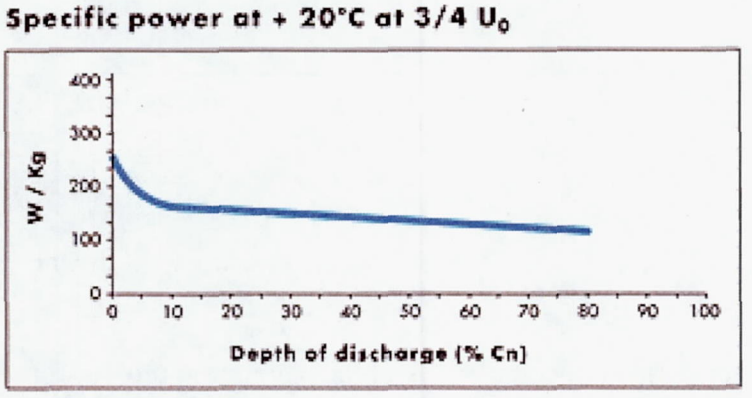

Figure 16 Effect of Depth of Discharge on Ni-Cad Battery Specific Power [3]

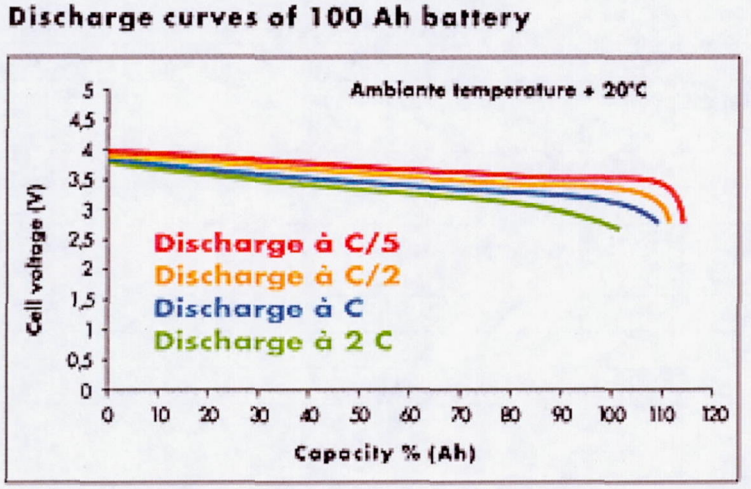

Figure 17 Effect of Discharge Rate on Li-Ion Battery Voltage [3]

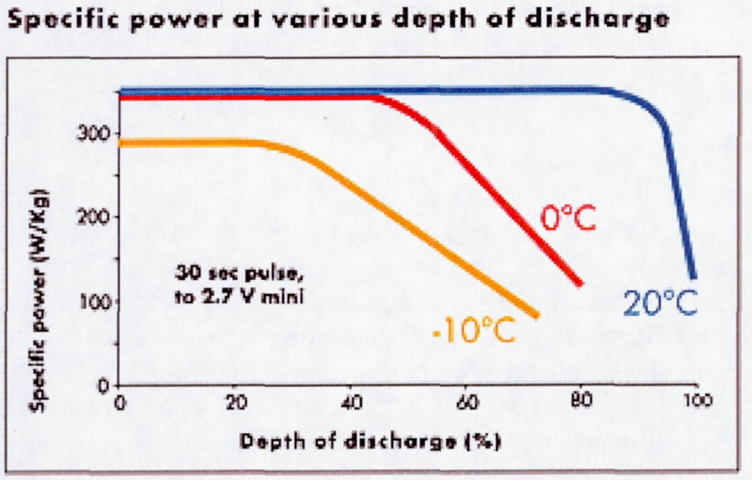

Figure 18 Effect of Depth of Discharge on Li-Ion Battery Specific Power [3]

Based on the data provided in Figures 15 and 16, the NiCd batteries discharge rate would be 2C. That is, the batteries would be drained at a rate that would fully discharge them in 30 minutes. Therefore since the operational time is 20 minutes and the battery capacity is 30 minutes the battery would need to have a 575 W-hr capacity. This provides a depth of discharge of 67%.

For the Li-Ion battery the desired depth of discharge would be 50%. To achieve this, the total capacity of the battery would need to be 766 W-hr, which translates into a discharge rate of 1.5C. The estimated battery performance specifications for both battery types are given in Table 3.

TABLE 3.—ESTIMATED PROPELLER BATTERY PERFORMANCE SPECIFICATIONS

Battery	Li-Ion	Ni-Cad
Operational Voltage per Cell	3.5 V	5.4 V
Depth of Discharge	50 %	67 %
Discharge Rate	1.5 C	2 C
Estimated Battery Specific Mass	131 Whr/kg	42 Whr/kg
Total Capacity Required	766 Whr	575 Whr
Estimated Mass	5.84 kg	12.7 kg
Estimated Volume	3060 cm^3	6600 cm^3

One of the main issues with the operation of the batteries is the temperature at which they will operate. Both high and low temperature extremes can be encountered during the experimental operation. Initially the batteries will be cold due to the slow ascent to the flight altitude. Ideally they would be insulated to maintain them at a temperature of 0 to 20 °C. However, during operation the insulation may cause the batteries to overheat since they will be drained at a fairly high rate which will cause significant internal heating. Experimentation will need to be performed in the Phase II portion of the program to determine the best thermal management scheme for the batteries.

Electric Motor

The power level at which the electric motor must operate at is on the high side for power levels of present day model aircraft. One of the motors looked at was the Aveox model 2315/8Y brushless DC electric motor. This motor represents the state-of-the-art in high power, model aircraft, electric motors. A brushless motor reduces the risk of arcing that may be seen with a brushed motor while operating at high power levels within a rarefied atmosphere. The Aveox motor is compact, lightweight and capable of delivering the power level required by the propeller. Its specifications are shown in Table 4.

However there are some significant drawbacks to the use of this type of motor. First is the ability to cool the motor. Because of its small size (and therefore small thermal mass) it will heat up very rapidly and will require cooling throughout its operation. Normally this would come from the air passing over the motor. However, since it will be operating at high altitudes, the convective cooling by the atmosphere may not be sufficient. A potential solution would be to place a sleeve over the motor that has fins for enhancing the heat transfer to the air stream. Another issue with the size of the motor is its ability to structurally hold the propeller secure. The motor only has a 5mm shaft diameter. Due to the large propeller size (1.5m diameter) there can be significant bending loads placed on this shaft. This increases the risk of a mechanical failure of the motor.

TABLE 4.—AVEOX BRUSHLESS DC MOTOR SPECIFICATIONS

Motor	Aveox 2315/8Y
Maximum Power	3500 W (for 30 Second Duration)
Maximum Continuous Power	2100 W (Cooling Dependent)
Maximum RPM	10,000
Dimensions	8.3 cm X 5.7 cm
Mass	0.85 kg
Torque / Amp	0.0516 N-m/amp 0.129 N-m/amp (geared)
Gear Box Ratio	2.5
Max Efficiency Operating Current	40 Amps
Max Efficiency Operating Voltage	43 Volts

The second issue is that the efficiency of this type of brushless motor decreases as the operating current increases. This can be seen in Figure 19. This decrease in efficiency is due mainly to the electronics needed in a brushless motor for it to operate. At higher current levels the efficiency of the control electronics decrease. Above about 20 amps conventional brushed motors tend to become more efficient than brushless motors. [4]

In order for the Aveox motor to turn the propeller at the desired RPM, a gearbox will be needed. The approximate gear ratio will be 3.5 to 1. Because of this unique application, a custom gearbox will need to be developed. The gearbox design will be driven by the high altitude environment in which it will operate. The major issues that need to be addressed for the successful design of a drive system are listed below.

- Cold soak during ascent
- Out-gassing restriction
- Oil-free operation
- Cooling restriction
- Low weight
- Speed ratio
- Dry lubricated bearings

If the Aveox motor or a similar type motor is used, the design process for the gearbox will take place during the Phase II portion of the program.

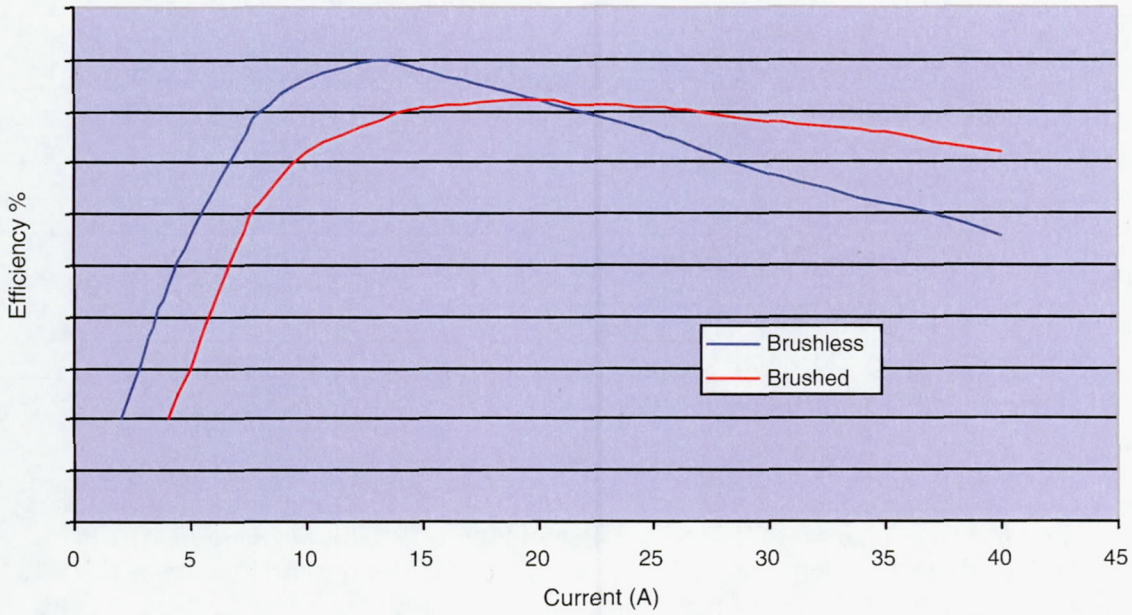

Figure 19 Typical Efficiency Trends for Brushed and Brushless DC Electric Motors

Because of the issues listed above, a brushed motor was also evaluated. The motor chosen is a lightweight high power density motor that was designed for electric vehicle operation. It is manufactured in England by the Lynch Motor Company. [5] This motor is a step up in power and size from those used in model aircraft. The motor mass is approximately 9 kg with a diameter of approximately 20 cm and a shaft diameter of 19mm. The motor performance curves are given in Figures 20 and 21. The motor is fairly easy to operate, the RPM is changed by varying the voltage to the motor through a motor controller. Because the motor's maximum RPM of 3900 is just above where the propeller will be operating no gearbox is needed.

The Lynch motor is a much more substantial and powerful motor which would provide a lot of margin during the propeller experiment. The motor should also be able to handle the thermal and mechanical environment better then the smaller Aveox motor. If the weight is not prohibitive this motor would pose less risk of failure during the experiment and would be the better choice. Prior to using this type of motor it would need to be tested under similar environmental conditions to ensure that it did not arc during operation.

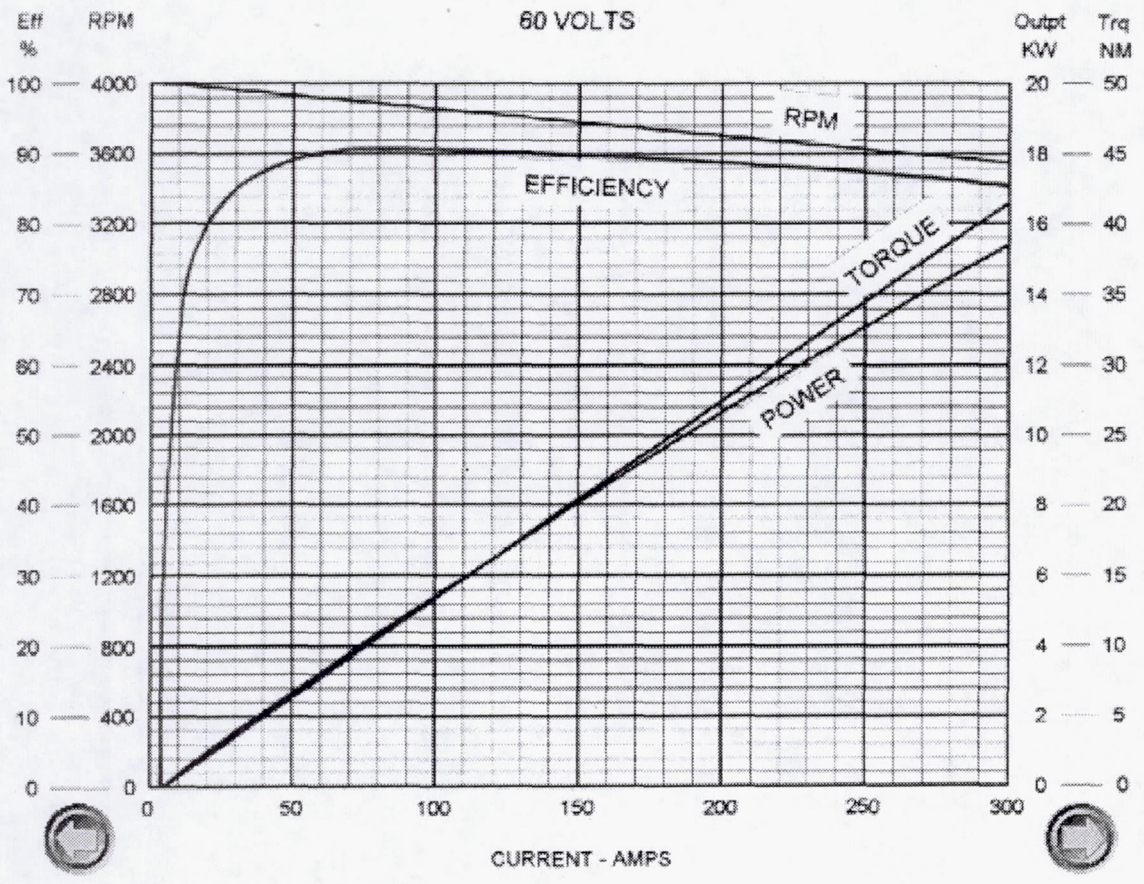

Figure 20 Performance Curves for Lynch Motor Operating at 60 V [5]

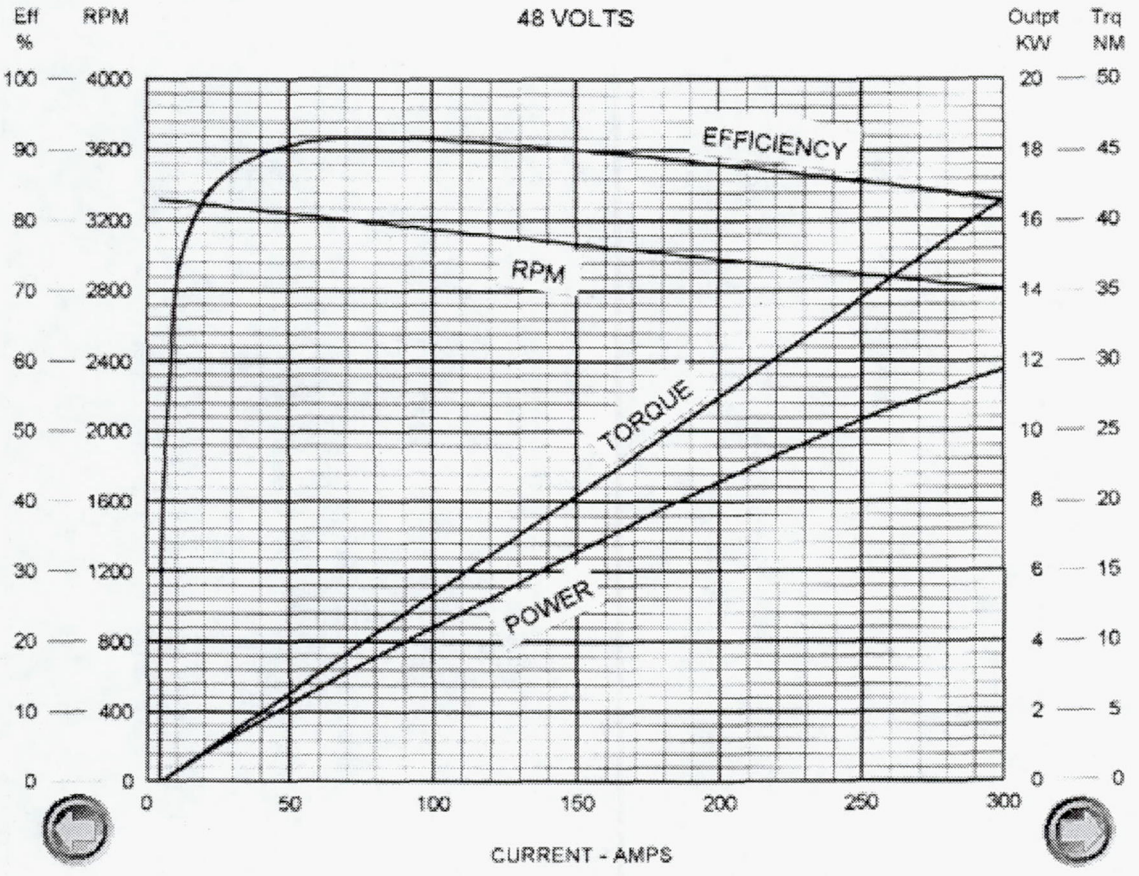

Figure 21 Performance Curves for Lynch Motor Operating at 48 V [5]

Motor Controllers

Presently Aveox does not have a controller that can be used with its 2315 motor at the power levels we are interested in. The controller would need to be custom made for this motor and optimized for minimum mass. However, since the current and power levels are fairly high, the optimization may not provide much of a mass benefit over the standard controller which would be used by the Lynch motor.

Permanent magnet motors like the Lynch motor are ideal for controlling RPM. Under no-load conditions the speed is directly proportional to the applied voltage. As load is applied the motor RPM will fall slightly. Speed control can be achieved by using a pulse width modulated (PWM) controller. A typical controller of this type would be a Curtis 1204, which has a mass of 2.27 kg.

Instrumentation and Data Collection

To determine propeller performance, data will be collected on the thrust and torque generated by the propeller as well as any blade aerodynamic data that can be obtained. The data to be collected will be generated by sensors on the electric motor, a thrust stand, instrumentation mounted within the propeller wake and on the blades themselves.

The instrumentation of the motor is a fairly straightforward process. A current sensor is placed around one of the power leads to the motor and voltage is measured across the power input terminals. Data on voltage and current is sampled by the data logging system. The output shaft of the motor will also be instrumented to measure RPM. This measurement will be accomplished through magnetic contact on the shaft and a magnetic pickup near the shaft. The propeller torque can be determined from the power input to the electric motor, the shaft RPM and characterized gearbox.

For the thrust measurement, a standard propeller thrust stand can be used. This consists of a flange that the propeller is mounted to. The flange is connected to the balance by an isolation cylinder. The balance consists of eight flexures that feed into a central hub. These flexures are monitored for movement via strain gauges. The drive shaft from the electric motor connects to the central hub of the force balance. A diagram of a typical thrust balance is shown in Figure 22.[6] As an added benefit, this force balance can also measure torque. This can provide a redundant means of measuring torque in addition to the input power and RPM method.

One issue with the thrust design that must be addressed is the propeller hub/nacelle orientation. Any spacing between the hub and the nacelle can cause a negative pressure to be generated behind the spinner. Since the thrust levels generated by the propeller are low this potential negative force could dramatically affect the thrust measurements, producing a significant underestimate of the thrust generated. This issue will need to be further addressed under the Phase II portion of the program.

Data can also be taken directly from the airflow over the propeller. Hot film or hot wire sensors can be place within the wake of the propeller. This can be done by either attaching them to a rake behind the blade (as shown in Figure 1) or by positioning them on a support behind the propeller. The main objective to this type of data collection would be to provide information on the drag produced by the propeller during operation. By attaching the sensors to the propeller blade, data can be gathered on the airfoil wake generated and provide insight to the airfoil and propeller drag. By sampling the wake behind the complete propeller an estimate of the overall propeller drag can be produced.

The main issue with using this type of sensor is whether or not they can be calibrated correctly. Calibration is crucial to producing useful data and since these sensors will be operating in a very low Reynolds number environment, calibration may be a significant issue. Also there is concern of the sensors breaking either prior to or during propeller operation. The viability of this type of sensor will need to be further investigated in the Phase II portion of the program. Testing and further analysis will need to be conducted

to determine if the implementation of this type of sensor will provide meaningful data on the propeller performance.

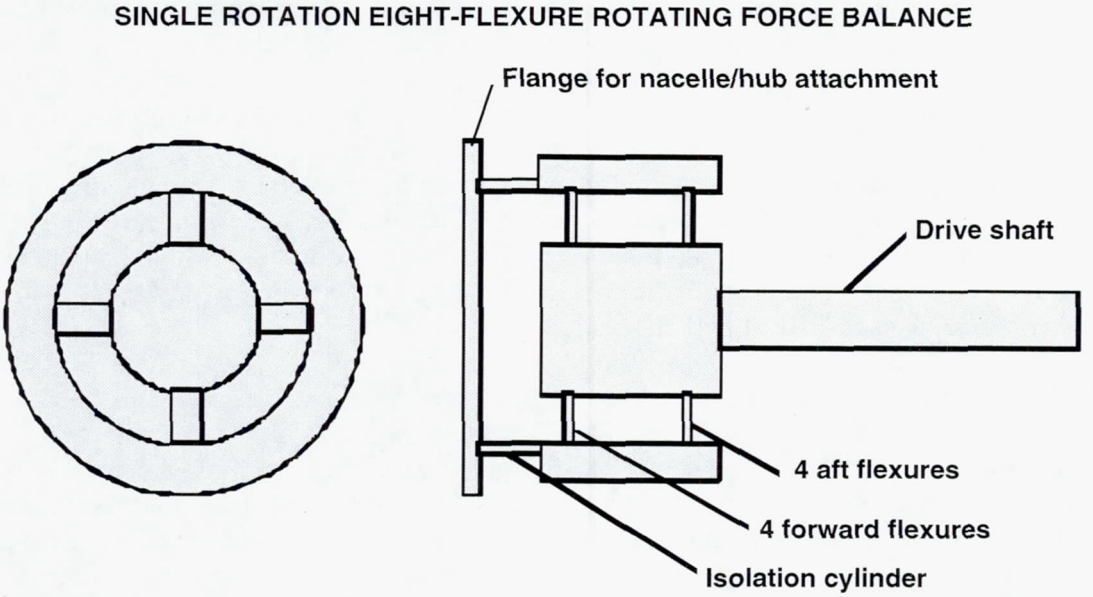

Figure 22 Thrust Balance Layout [6]

Any data collected off of the propeller blades themselves will need to be relayed back to the data collection system within the APEX vehicle. Presently there are two approaches being considered to accomplish this. The first would be to use a slip ring on the propeller shaft that can provide a data link back to the data logging system. An optical slip ring would provide the greatest data transfer capability while minimizing electronic noise. The other option is to place a small transmitter and battery within the spinner of the propeller. Since the transmission distance is small, the power required by the transmitter should be relatively small, on the order of a few watts. A receiver in the APEX vehicle would pick up the signal from the transmitter and send the data to the data logger. The main issue with this data transmission system would be RF noise that is generated either by the experiment or by some other device on the APEX vehicle. Any significant RF noise could potentially eliminate or severely reduce the data collected.

Visual data on the propeller operation is also desirable. This would consist of a video image of the propeller operating from the edge of the propeller disc. This would show any flexing of the propeller during operation.

Summary

As shown in Figure 1 the high altitude propeller test consists of the propeller, electric motor, controller, batteries, thrust stand, various sensors and structural support. This preliminary design was performed in order to determine what the data generating capabilities of such an experiment might be as well as what impact it would have on the APEX vehicle.

From the analysis that was performed, it was determined that the propeller would run over a range of Reynolds numbers (~ 30,000 to ~150,000) that would be desirable to investigate. The thrust produced by the propeller would be representative of that which would be expected for a Mars-based aircraft. Also the experiment run time is more than sufficient to get a very good representation of the propeller operation as well as being representative of the duration of a battery-powered Mars aircraft flight. By providing this extensive run time, the experiment not only examines the propeller performance but it also can be used as a means for evaluating the complete power system for a potential Mars aircraft. A number of the issues that will need to be addressed in getting the power system to operate for this experiment will be directly applicable to the design of a power system for an electric Mars aircraft.

TABLE 5.—MASS ESTIMATES FOR THE VARIOUS SYSTEM COMPONENTS

Component	Conservative	High Performance
Propeller Blades	Aluminum 2.36 kg	Carbon 1.16 kg
Propeller Hub	~1.50 kg	~1.00 kg
Electric Motor	9.00 kg	1.00 kg
Gearbox	NA	2.00 kg
Motor Thermal Control	NA	~1.50 kg
Motor Controller	2.27 kg	~1.50 kg
Sensor System (rake)	~0.50 kg	~0.50 kg
Batteries	Ni-Cad 12.70 kg	Lithium Ion 5.84 kg
Thrust Stand	~2.00 kg	~1.00 kg
Structure	~8.00 kg	~5.00 kg
Misc. Items and Margin (10%)	~3.83 kg	~2.05 kg
Total	42.4 kg	22.55 kg

An estimate of the mass of the experiment system was produced. Since the mass of this system can have a fairly large impact on the APEX vehicle, two different components were investigated for some of the items used in the experiment. These were either "conservative" based on off-the-shelf components with capabilities beyond that required by the experiment or "aggressive" using made-to-order components that are sized to just meet the system requirements. In general, this is the approach that can be taken of the system as a whole. The more lightweight, custom components which are used, the lighter the system but the greater the cost and operational risk. Table 5 shows a mass comparison

between a conservative system and a higher performance system. It should be noted however that the components on the table can be intermixed to produce the most desirable system.

In the next phase of this program the items addressed in this preliminary experiment design will be expanded upon to provide a working experiment package that meets the goals of the experiment as well as the capabilities of the APEX vehicle. This preliminary design was performed to determine the feasibility of this experiment as well as estimate its requirements. The main items that will need to be addressed in the follow on effort are outlined below.

- Detailed system design, layout and integration drawings
- Detailed propeller design, including hub and mounting scheme
- Gearbox design (if needed)
- Motor controller design (if needed)
- Thrust stand design and verification testing
- Operational control system programming including: startup, operation, shutdown and emergency shutdown procedures
- Wake sensor rake design and calibration testing
- Nacelle structural design
- Sensor integration (voltage, current , RPM) and environmental testing/calibration
- Experimental Testing of Components
  - Battery operation and thermal testing
  - Electric motor environmental testing
  - Gearbox environmental testing (if needed)

Operational Risks and Interaction with the Aircraft

There are risks associated with running any experiment, especially a dynamic one such as a propeller test. The main risk associated with this experiment is the structural or mechanical failure of one of the main components. The most devastating failure would be if one of the propeller blades broke off during operation. The hazards here would be the potential direct impact of the blade onto the APEX vehicle as well as the out-of-balance loads transmitted to the test pylon and aircraft structure. These loads could cause damage as well as loss of control of the vehicle. There can be a number of causes for a blade failure. The most likely would be a defect in manufacturing that produces a reduction in strength or a stress concentration point. Another mode of failure would be fluttering of the propeller blade during operation. This could cause a catastrophic failure of the propeller. Fluttering could be induced by aerodynamic forces combined with a flexible structural design or can be set up by shock formation and shedding off of the propeller tips. If the structurally rigid blade, as suggested previously, is utilized this will substantially reduce the risk of flutter. Also the aircraft speed and propeller RPM can be controlled to ensure that the blade tips do not exceed some pre-designated subsonic mach number.

Another major risk associated with this system is the loss of thermal control. Due to the fairly large amount of power required to operate the propeller over a relatively short period of time, there will be a significant amount of heat that must be dissipated from the system. The main heat-generating components will be the batteries and the motor/controller. If cooling to these systems is blocked or not adequate, then these components could fail, resulting in propeller damage or, potentially, a fire.

The propeller during operation can impart some forces onto the aircraft. One of these would be a gyroscopic force due to the movement of the axis of rotation of the propeller. Since the propeller is a rotating device, it will exert gyroscopic forces and moments whenever its axis of rotation is moved due to the aircraft pitch or yaw maneuvers. However, the rate of these motions is fairly small and therefore the subsequent gyroscopic forces generated by the propeller should not be a stability issue for the aircraft. [7]

Propeller vibration, if it becomes excessive, can also be of concern to the aircraft. The main source of vibration which can lead to propeller blade flutter is the periodic changing of the lift and drag forces on the propeller blades. This can occur from a change in air velocity over the propeller blades as it rotates. This situation could be due to an obstruction upstream of the propeller that interferes with the free stream flow to the propeller. The most effective way to avoid this is by making sure the free stream path to the propeller is clear of obstacles.

Vibration can also be due to harmonic loading. This loading of the propeller blade occurs once per revolution and is approximately proportional to angle of attack of the propeller relative to the free stream and the airplane dynamic pressure. This harmonic loading will be strongest when the aircraft is at its highest angles of attack, during release from the balloon and climb out. However since there is no plan to operate the propeller during this portion of the flight and because of the very low air density (and hence dynamic pressure) at the testing altitude, harmonic loading should not be an issue.

References

1. Greer, D., Hamory, P., Krake, K. and Drela, M.: "Design and Predictions for a High-Altitude (Low-Reynolds-Number) Aerodynamic Flight Experiment", NASA TM—1999-206579, July 1999.

2. Selig, M.S., Donovan, J.F., and Fraser, D.B.: "Airfoils at Low Speeds", Soartech 8, 1989.

3. Battery Data Sheets, Saft America, Inc., Valdosta, Georgia, 31601

4. Boucher, Robert J.,"Electric Motor Handbook," AstroFlight, Inc., 1995.

5. Lynch Motor Company, "Performance Specifications and Curves," http://www.lynchmotor.com.

6. Jeracki, R.J., "NASA Lewis Experience With Force Balances for Scale Model Engine Performance Measurement in Wind Tunnels," Internal NASA Glenn Research Center Memo, January 1994.

7. Amatt, W., et al, "Summary of Propeller Design Procedures and Data. Volume II, Structural Analysis and Blade Design," USAAMRDL Technical Report 73-34B, November 1973.

Appendix A

SD8000-PT AIRFOIL COORDINATE POINTS NORMALIZED TO A CHORD LENGTH OF 1

	Upper Half of Airfoil			Lower Half Of Airfoil	
	X	Y		X	Y
1	1.00000	0.00000	25	0.00102	-0.00319
2	1.00046	0.00111	26	0.00371	-0.00622
3	0.99665	0.00195	27	0.00922	-0.00961
4	0.98897	0.00307	28	0.01796	-0.01358
5	0.96936	0.00554	29	0.02842	-0.01697
6	0.93466	0.01027	30	0.04584	-0.02041
7	0.89450	0.01624	31	0.07055	-0.02359
8	0.82036	0.02689	32	0.11413	-0.02689
9	0.75841	0.03476	33	0.16687	-0.02834
10	0.70380	0.04128	34	0.22209	-0.02834
11	0.64809	0.04662	35	0.29657	-0.02675
12	0.57198	0.05264	36	0.36217	-0.02436
13	0.48977	0.05786	37	0.43854	-0.02091
14	0.40596	0.06130	38	0.53740	-0.01575
15	0.32881	0.06252	39	0.62509	-0.01101
16	0.25288	0.06117	40	0.70568	-0.00666
17	0.17660	0.05690	41	0.78624	-0.00248
18	0.11169	0.04938	42	0.87495	0.00048
19	0.05866	0.03824	43	0.93423	0.00087
20	0.03413	0.02978	44	0.97424	-0.00016
21	0.01668	0.02080	45	0.99198	-0.00099
22	0.00800	0.01455	46	0.99724	-0.00115
23	0.00318	0.00899	47	0.99949	-0.00113
24	0.00000	0.00000	48	1.00000	0.00000

REPORT DOCUMENTATION PAGE

Form Approved
OMB No. 0704-0188

1. AGENCY USE ONLY (Leave blank)	2. REPORT DATE	3. REPORT TYPE AND DATES COVERED
	September 2002	Final Contractor Report

4. TITLE AND SUBTITLE

APEX 3D Propeller Test Preliminary Design

5. FUNDING NUMBERS

WU–708–87–13–00
NAS3–00145

6. AUTHOR(S)

Anthony J. Colozza

7. PERFORMING ORGANIZATION NAME(S) AND ADDRESS(ES)

Analex Corporation
3001 Aerospace Parkway
Brook Park, Ohio 44142

8. PERFORMING ORGANIZATION REPORT NUMBER

E–13539

9. SPONSORING/MONITORING AGENCY NAME(S) AND ADDRESS(ES)

National Aeronautics and Space Administration
Washington, DC 20546–0001

10. SPONSORING/MONITORING AGENCY REPORT NUMBER

NASA CR—2002-211866

11. SUPPLEMENTARY NOTES

Project Manager, Lisa Kohout, Power and On-Board Propulsion Technology Division, NASA Glenn Research Center, organization code 5420, 216–433–8004.

12a. DISTRIBUTION/AVAILABILITY STATEMENT

Unclassified - Unlimited
Subject Category: 07 Distribution: Nonstandard

Available electronically at http://gltrs.grc.nasa.gov

This publication is available from the NASA Center for AeroSpace Information, 301–621–0390.

12b. DISTRIBUTION CODE

13. ABSTRACT ***(Maximum 200 words)***

A low Reynolds number, high subsonic mach number flight regime is fairly uncommon in aeronautics. Most flight vehicles do not fly under these aerodynamic conditions. However, recently there have been a number of proposed aircraft applications (such as high altitude observation platforms and Mars aircraft) that require flight within this regime. One of the main obstacles to flight under these conditions is the ability to reliably generate sufficient thrust for the aircraft. For a conventional propulsion system, the operation and design of the propeller is the key aspect to its operation. Due to the difficulty in experimentally modeling the flight conditions in ground-based facilities, it has been proposed to conduct propeller experiments from a high altitude gliding platform (APEX). A preliminary design of a propeller experiment under the low Reynolds number, high mach number flight conditions has been devised. The details of the design are described as well as the potential data that will be collected.

14. SUBJECT TERMS

Propellers; Propeller efficiency; Propulsion system performance; High altitude flight

15. NUMBER OF PAGES

36

16. PRICE CODE

17. SECURITY CLASSIFICATION OF REPORT	18. SECURITY CLASSIFICATION OF THIS PAGE	19. SECURITY CLASSIFICATION OF ABSTRACT	20. LIMITATION OF ABSTRACT
Unclassified	Unclassified	Unclassified	